Monthly Notices
of the
ROYAL ASTRONOMICAL SOCIETY

MNRAS **474,** 3162–3172 (2018)
Advance Access publication 2017 October 5

doi:10.1093/mnras/stx2561

Redshift determination of the BL Lac object 3C 66A by the detection of its host galaxy cluster at $z = 0.340$ ⋆

Juanita Torres-Zafra,[1,2†] Sergio A. Cellone,[1,2‡] Alberto Buzzoni,[3] Ileana Andruchow[1,2] and José G. Portilla[4]

[1] *Instituto de Astrofísica de La Plata (CCT La Plata-CONICET-UNLP), Paseo del Bosque, B1900FWA, La Plata, Argentina*
[2] *Facultad de Ciencias Astronómicas y Geofísicas, Universidad Nacional de La Plata, Paseo del Bosque, B1900FWA La Plata, Argentina*
[3] *Osservatorio Astronomico di Bologna (INAF), Via Ranzani 1, I-40127 Bologna, Italy*
[4] *Universidad Nacional de Colombia (UNal), 111321 Bogotá, Colombia*

Accepted 2017 September 28. Received 2017 September 28; in original form 2016 August 5

ABSTRACT

The BL Lac object 3C 66A is one of the most luminous extragalactic sources at TeV γ-rays (very high energy, i.e. $E > 100$ GeV). Since TeV γ-ray radiation is absorbed by the extragalactic background light (EBL), it is crucial to know the redshift of the source in order to reconstruct its original spectral energy distribution, as well as to constrain EBL models. However, the optical spectrum of this BL Lac is almost featureless, so a direct measurement of z is very difficult; in fact, the published redshift value for this source ($z = 0.444$) has been strongly questioned. Based on EBL absorption arguments, several constraints to its redshift, in the range $0.096 < z < 0.5$, were proposed. Since these active galactic nuclei (AGNs) are hosted, typically, in early-type galaxies that are members of groups or clusters, we have analysed spectro-photometrically the environment of 3C 66A, with the goal of finding the galaxy group hosting this blazar. This study was made using optical images of a 5.5×5.5 arcmin^2 field centred on the blazar, and spectra of 24 sources obtained with Gemini/GMOS-N multi-object spectroscopy. We found spectroscopic evidence of two galaxy groups along the blazar's line of sight: one at $z \simeq 0.020$ and the second one at $z \simeq 0.340$. The first one is consistent with a known foreground structure, while the second group presented here has six spectroscopically confirmed members. Their location along a red sequence in the colour–magnitude diagram allows us to identify 34 additional candidate members of the more distant group. The blazar's spectrum shows broad absorption features that we identify as arising in the intergalactic medium, thus allowing us to tentatively set a redshift lower limit at $z_{3C66A} \gtrsim 0.33$. As a consequence, we propose that 3C 66A is hosted in a galaxy that belongs to a cluster at $z = 0.340$.

Key words: BL Lacertae objects: individual: 3C66A – galaxies: clusters: general – galaxies: distances and redshifts.

1 INTRODUCTION

Blazars are the class of active galactic nuclei (AGNs) which display the most extreme properties: strong and highly variable emission across the entire electromagnetic spectrum, from radio to gamma-rays, reaching in some cases the very high energy (VHE; i.e. $E > 100$ GeV) domain (Urry & Padovani 1995). It is widely accepted that a blazar's observed radiation arises from a relativistic jet pointing at small angles with respect to our line of sight. The spectral energy distribution (SED) of these sources is thus dominated by non-thermal radiation, showing two bumps: the low-frequency one (from radio to X-rays) is ascribed to synchrotron emission, while the bump at high frequencies (X-rays to γ-rays) is likely produced by inverse-Compton scattering (Konigl 1981).

Blazars are classified based on the specific characteristics of their optical spectra. In this way, objects with significant emission-line equivalent widths ($|EW| > 5$ Å, rest frame) are called flat-spectrum radio quasars (FSRQs), while those without (or with weak) emission lines are called BL Lac objects. The featureless continua that – by definition – characterize the optical spectra of the latter, in many cases prevent the determination of their redshifts. Nevertheless, a

⋆ Based on observations carried out at the 8.1 m telescope of Gemini North Observatory, Mauna Kea (Hawaii, USA).

† E-mail: jtzafra@fcaglp.unlp.edu.ar
‡ Current affiliation: Complejo Astronómico El Leoncito (CASLEO), CONICET-UNLP-UNC-UNSJ, Argentina

precise knowledge of the distances of these objects is mandatory for constraining models of their emission, considering also that these sources are the dominant population of the extragalactic sky at high energies (Costamante 2013). In the absence of direct (i.e. spectroscopic) redshift measurements, other indirect procedures have been proposed to estimate, or at least constrain, BL Lac's redshifts.

One of them uses the blazar's host galaxy as a standard candle. Observations – particularly those performed with the *Hubble Space Telescope (HST)* – have shown that BL Lac objects are, almost always, found in elliptical galaxies; often luminous ellipticals comparable to brightest galaxies in small clusters or groups of galaxies (Urry et al. 2000). Sbarufatti et al. (2005) give, for BL Lac host galaxies, a mean absolute magnitude $M_{\rm R} = -22.9$, with a very low dispersion (± 1 mag), and a mean effective radius $R_{\rm eff} = 10$ kpc. Shaw et al. (2013), on the other hand, say that when the sample is limited to γ-emitting BL Lacs, the hosts seem to be $\sim$0.4 mag fainter: $M_{\rm R} = -22.5$ mag. Thus, the photometric (non-)detection of the host galaxy is used to set limits to the blazar's distance. Alternatively, a similar approach can be made through optical spectra, where the absence of host galaxy absorption lines (e.g. Landoni et al. 2014) or the detection of foreground absorptions (e.g. Landt 2012) set lower limits to a BL Lac's redshift.

The study of the TeV spectra of blazars can also provide redshift limits. Commonly, for large values of z, VHE gamma-rays are absorbed by the infrared component of the extragalactic background light (EBL), since its photons are annihilated via pair-production ($\gamma_{\rm VHE} + \gamma_{\rm EBL} \rightarrow {\rm e}^+ + {\rm e}^-$; Gould & Schréder 1967). This causes a decrease in the observed flux and a softening of the measured spectrum. The optical depth ($\tau(z, E)$) can be calculated if a model of the EBL is available, along with the redshift (z) and the gamma-ray photons energy (E). In this way, τ depends both on the distance travelled by the gamma-ray photon and its energy (Stecker et al. 1992), therefore, the knowledge of this parameter can be used to estimate the intrinsic flux of the source, once de-absorbed. Conversely, if an EBL model and an intrinsic gamma-ray SED are assumed, the redshift can be estimated (Prandini et al. 2010).

3C 66A is a well-studied blazar; it was classified as a BL Lac object by Maccagni et al. (1987), based on its significant optical and X-ray variability, and was detected at VHE gamma-rays by the Very Energetic Radiation Imaging Telescope Array System (VERITAS) (Acciari et al. 2009). The synchrotron peak of this source is located between 10^{15} and 10^{16} Hz (Perri et al. 2003), therefore it can also be classified as an intermediate-frequency peaked BL Lac object (IBL) or an intermediate synchrotron-peaked (ISP) blazar.

An accurate determination of z is crucial to obtain the original photon spectrum of the source. The VHE gamma-ray flux of distant sources, such as 3C 66A should the assumed $z = 0.444$ be real, is expected to be significantly suppressed. Even assuming a smaller value for z, the total amount of gamma-ray flux emitted, calculated following the prescription of Mazin & Raue (2007) for 3C 66A, must be huge and with a very hard spectrum (Aliu et al. 2009). Hence, verification of the actual redshift of the source is of importance both for AGN astrophysics and cosmology, therefore, several efforts have been made to determine this physical parameter.

The published redshift of this blazar was determined to be $z = 0.444$ from optical spectroscopy by Miller et al. (1978), based on the detection of one single line, however, the authors stated that they were not sure of the reality of this emission feature and warned that the redshift value is not reliable. Lanzetta et al. (1993) claimed a confirmation of the $z = 0.444$ value, based on data from the *International Ultraviolet Explorer* (*IUE*). Only one emission line was marginally detected and systematic errors affecting such detections could not be ruled out completely. This z value was questioned by Bramel et al. (2005), who encouraged further spectroscopic observations of this source. Another observation of 3C 66A at a different spectral range was reported by Finke et al. (2008), but no spectral feature was found; a lower limit for its redshift was thus set at $z \geq 0.096$. On the other hand, Wurtz et al. (1996) reported a marginal photometric detection of 3C 66A's host galaxy setting a lower limit to its redshift at $z > 0.321$.

More recently, by assuming that the EBL-corrected TeV spectrum is not harder than the *Fermi*–LAT spectrum, Prandini et al. (2010) suggested an upper limit $z < 0.34 \pm 0.05$ for the redshift of 3C 66A, with its most likely value being $z = 0.213 \pm 0.05$. Also, based on EBL absorption of 3C 66A's VHE spectrum, Yang & Wang (2010) set $z < 0.58$, while Yan et al. (2013) obtained $0.15 \leq z \leq 0.31$, with a best-fitting value $z = 0.21$. Finally, Furniss et al. (2013) reported a firm lower limit of 3C 66A's redshift at $z \geq 0.3347$, while a 99.9 per cent confidence upper limit was set at $z < 0.41$. These results are based on far-ultraviolet spectra (1132–1800 Å) obtained with the Cosmic Origins Spectrograph (COS) on-board *HST*, where intergalactic medium absorption features were detected on a smooth continuum.

An independent approach to find out the redshift of a BL Lac with a featureless optical spectrum is to search its (projected) neighbourhood for a group or cluster of galaxies, to which the blazar might be associated. Although several works have undertaken the study of the immediate environment of BL Lacs (Farina et al. 2016, and references therein), the use of the group/cluster redshift as a proxy for the blazar's redshift has been scarcely used (Pesce et al. 1995; Muriel et al. 2015; Rovero et al. 2016) (see also Torres Zafra et al. 2013, for preliminary results from the present project).

In particular, the galaxy environment of 3C 66A was tested by Butcher et al. (1976, hereafter But76), who found 15 probable members of a cluster surrounding 3C 66A, from which they estimated a photometric redshift $z \approx 0.37^{+0.07}_{-0.03}$. Later, and using the luminosity function of field galaxies, Wurtz et al. (1993) suggested that the blazar is associated to a poor cluster with a loosely constrained redshift $0.3 \leq z \leq 0.5$. Bowen et al. (1997, hereafter Bow97), in turn, provided redshifts between $z = 0.0198$ and 0.0675 for seven galaxies within a 16.7 arcmin^2 projected area centred on 3C 66A, however, these objects are relatively bright and none of them is included among the cluster member candidates cited above.

Considering the controversy about the redshift of 3C 66A, we have studied its environment using deep, two-colour photometry of 300 objects within a field centred on the blazar, and spectra of a sub-sample of 24 objects (down to $g' = 22.6$ mag, and including 3C 66A itself), obtained with the Gemini North Telescope and the Gemini Multi-Object Spectrograph (GMOS). Our goal is to look for both photometric and spectroscopic signatures of a group or cluster of galaxies hosting the blazar, thus providing an independent and reliable determination of its redshift.

This paper is structured as follows. In Section 2, the photometric and spectroscopic data are described. Section 3 presents data analysis and results, and in Section 4 the work is summarized and our conclusions are presented. In this paper, we assume a concordance cosmology with $H_0 = 69.6$ km s^{-1} Mpc^{-1}, $\Omega_{\rm m} = 0.286$ and $\Omega_\Lambda = 0.714$.

2 OBSERVATIONS AND DATA ANALYSIS

Observations were made at the 8.1 m Gemini North Telescope, Mauna Kea, Hawaii (USA), in 2009 August, using the GMOS instrument in both image and MOS modes (programme

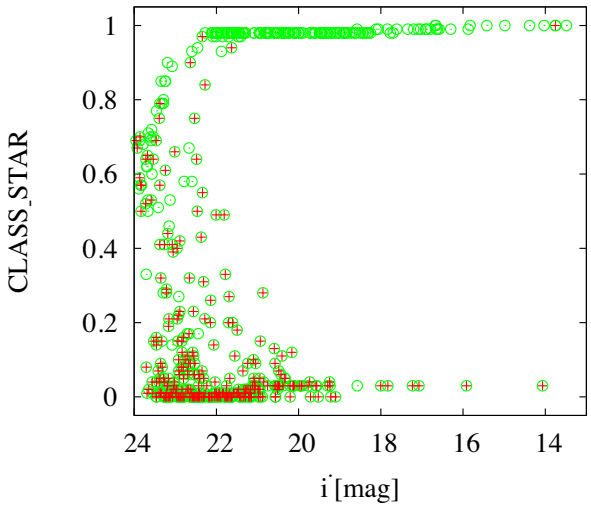

Figure 1. SExtractor classifier (*CLASS_STAR*) as a function of the apparent magnitude i' of all the sources detected in the field of 3C 66A (green circles). *CLASS_STAR* = 1: point sources; *CLASS_STAR* = 0: extended sources. Galaxies detected in the field having *FWHM* > 8 pixels in the i'-band (plus the blazar, the $i' \approx 14$ object with *CLASS_STAR* ≈ 1) are shown with red crosses.

GN-2009B-Q-2; PI: I. Andruchow). The details on these data and their reduction process are given below.

2.1 Images

Observations included images in the g' (475 nm) and i' (780 nm) bands, covering a field of 5.5 × 5.5 arcmin^2 centred on the blazar. Seeing *FWHM* was about 0.7 arcsec, and we chose to use no binning (thus giving a scale of 0.0727 arcsec pix^{-1}), to avoid saturation of the AGN, while getting sufficient S/N on the field galaxies. For the same purpose, we took several short-exposure frames through each filter: 11 × 120 s and 13 × 25 s in g' and i', respectively.

Images were bias-subtracted and flat-fielded with dome flats. Overall, data reduction was performed with tasks from the GEMINI.GMOS package included in IRAF[1].

We performed photometry on the images using SExtractor (Bertin & Arnouts 1996). This software allows to identify and classify point and extended sources, building catalogues with several photometric parameters. The *MAG_AUTO* parameter was used to measure total magnitudes of all the objects detected in the field, with an average error of ±0.005 mag for the brightest sources ($g' < 21$) and ±0.026 mag for the faintest sources ($g' > 23$). The *CLASS_STAR* parameter, in turn, allowed us to identify the galaxies. This classification was further verified from the PSF (Point Spread Function) of the sources, discarding those showing a brightness profile with *FWHM* ≤ 8 pixels in the i'-band. In this way, we could discriminate, with greater certainty, extended sources presenting intermediate classifications with *CLASS_STAR* (see Fig. 1). A visual inspection of the identified extended objects was performed, discarding those which were found to be saturated point sources, CCD blemishes, etc.

Magnitudes were corrected for Galactic extinction with the values from Schlafly & Finkbeiner (2011), as given in NASA Extragalactic Database (NED)[2]. We compared our photometry with several field stars in common with González-Pérez et al. (2001), obtaining fairly good agreement. The apparent magnitudes for 3C 66A were then measured to be $g' = 14.32$ and $i' = 13.75$ mag. In Fig. 1, we plot the classification parameter *CLASS_STAR* as a function of the i' magnitude for all sources detected in the field of 3C 66A. On the same diagram, we plotted extended objects identified from the *FWHM* > 8 pixels criterion, which were selected for this research.

The objects selected within the field for further photometric analysis were those brighter than 24.5 mag in the g'-band.

2.2 Spectra

Spectroscopic data were acquired in the multi-object (MOS) mode, making use of two diffraction gratings: *B*600_*G*5307 and *R*400_*G*5325. Two multislit masks (one for each grating) were created from a co-added image provided by Gemini from our photometric images (see Section 2.1). The final mask for the B600_G5307 grating consisted of 23 slits with dimensions of 1.5 arcsec by 8 arcsec, whereas for the *R*400_*G*5325 grating it consisted of 11 slits with dimensions of 1 arcsec by 8 arcsec. Slits were placed prioritizing faint non-stellar objects in the usable field. Six exposures of 1800 s each were obtained with the *B*600_*G*5307 grating (with a binning of 2 × 2) in three different central wavelengths: 490, 500 and 510 nm, to remove the gaps between the CCDs. The wavelength range covered was 3500–6500 Å with a spectral resolution of 0.54 nm. The *B*600_*G*5307 mask allowed us to extract the spectra of 23 objects.

The *R*400_*G*5325 grating was used in the MOS+N&S mode, covering a wavelength range of 7000–10 000 Å with a spectral resolution of 0.79 nm. Eight exposures of 500 s each were obtained (with a binning of 2 × 2) in three different central wavelengths: 790, 800 and 810 nm. The *Nod&Shuffle* (N&S) mode was used to optimally subtract the sky (Glazebrook & Bland-Hawthorn 2001), which is a particularly important issue in the redder range. Unfortunately, an error during the observations design led to partial overlapping of the resulting spectra, so we were only able to extract the spectra of four objects in this mask (of these, three were also observed through the *B*600_*G*5307 mask). The objects with spectroscopic data in the field (with at least one grating) are shown in Fig. 2.

The spectroscopic data reduction was also performed with standard IRAF procedures within the GEMINI package, namely: GBIAS, GSFLAT, GSREDUCE, GSMOSAIC and GSCUT. Pixel to wavelength transformation was established using GSTRANSFORM, from CuAr lamps spectra obtained as daytime calibrations. Finally, the individual spectra were extracted with GSEXTRACT. As redshift determination was our main goal, no flux calibration was performed on the extracted spectra.

This procedure was followed on data obtained in both observing modes, however, additional tasks (GNSSKYSUB and GNSCOMBINE) were necessary for the subtraction of the sky and the combination of spectra taken in the N&S mode.

[1] IRAF is distributed by the National Optical Astronomy Observatories, which are operated by the Association of Universities for Research in Astronomy, Inc., under cooperative agreement with the National Science Foundation.

[2] https://ned.ipac.caltech.edu/. The NASA/IPAC Extragalactic Database (NED) is operated by the Jet Propulsion Laboratory, California Institute of Technology, under contract with the National Aeronautics and Space Administration.

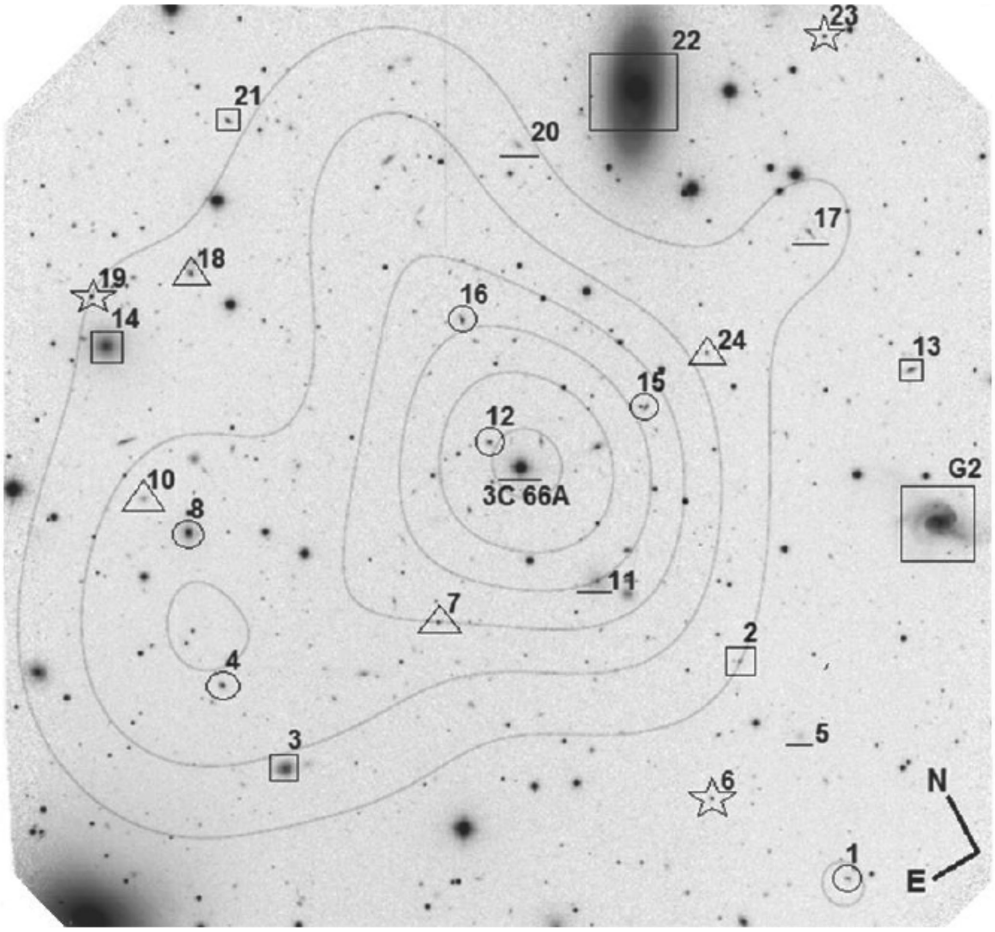

Figure 2. GMOS i'-band image of the field centred on 3C 66A. Spectroscopically observed objects are labelled following their slit number and marked according to their redshift (see Table 1), with respect to the detected $z = 0.340$ group (see Section 3.1): triangles ($z > 0.340$), circles ($z \simeq 0.340$), squares ($z < 0.340$), star shape (Galactic stars) and straight lines underneath (objects with unknown redshift). The large boxes mark galaxies G1 (slit #22) and G2 in Bowen et al. (1997). Contours show the projected density of candidate members of the $z = 0.340$ group (see the text). The frame is 5.5 arcmin on a side, corresponding to 1.61 Mpc at $z = 0.340$.

Cosmic rays cleaning was performed following the routine given in the GSCRSPEC.CL script, available at the Gemini Observatory website[3]. This script uses the *Laplacian Cosmic Ray Identification* method developed by Pieter G. van Dokkum in the LACOS_SPEC.CL script[4]. We verified that this procedure is more efficient than the IRAF task GSCRREJ to clean cosmic rays.

We then used the FXCOR task to determine the redshifts of selected objects in the field. This task allows to calculate the radial velocity through Fourier cross-correlation between the spectrum of the object under analysis and a reference (template) spectrum (Tonry & Davis 1979). Both spectra are continuum subtracted and Fourier filtered before doing the correlation, while dispersions are equalized by rebinning to the smallest dispersion. For this work, we used two reference spectra: that of NGC 4449 (Kennicutt 1992), an irregular galaxy that has well-defined emissions, and the spectrum of NGC 4387 (Gavazzi et al. 2004), an elliptical galaxy showing strong absorptions. Both templates were downloaded from NED. For those spectra where it was possible to establish a tentative redshift value, typical emission lines were identified, such as H γ, [O II] (3727 Å), H β, [O III] (4959 Å) and [O III] (5007 Å), and/or absorptions, like Ca II (H+K), Ca+Fe, Na I and H α. Finally, the redshift adopted for each object was computed from Gaussian fits to two or more such features in its spectrum. Three objects (slits #6, #19 and #23) turned out to be Galactic stars[5] (we give their radial velocities in Table 1), while no reliable redshift value could be obtained for other five objects (slits #5, #11, #13, #17 and #20), due to the low S/N ratio of their spectra (we will return to objects #5 and #11 in Section 3.2). Tentative redshifts for two of them (slits #17 and #20) were measured through just one emission line each, which we assumed to be [O II] (3727 Å) and H δ, respectively (based on their colours and spiral morphology). So, their tentative redshift values would be $z_{\#17} \simeq 0.476$ and $z_{\#20} \simeq 0.479$. No clear emission or absorption lines could be identified in the blazar's spectrum, besides telluric lines and diffuse interstellar bands (DIBs), so no definite redshift value could be established in this way for 3C 66A (see, however, Section 3.3 for our analysis on probable foreground absorptions on the blazar's spectrum). Redshifts were thus established for 15 (plus two just tentative) out of the 24 selected objects. Our

[3] http://www.gemini.edu/sciops/data/software/gscrspec.cl
[4] http://www.astro.yale.edu/dokkum/lacosmic/lacos_spec.cl.

[5] The spectrum of object #6 looks like that of a red dwarf star, possibly blended with a hotter component. Given its magnitude ($g' \simeq 21$ mag), it should then be a very distant (≈30 kpc) halo star.

Table 1. Spectro-photometric results for selected objects in the field of 3C 66A: col. 1: slit number; col. 2: identification label (ID), either from this paper or from other works; cols. 3 and 4: RA and Dec. (J2000); cols. 5 and 6: g' and i' total integrated magnitude; col. 7: redshift (z), or radial velocity (for Galactic stars); col. 8: object type.

Slit	ID	RA_{J2000} (hh:mm:ss)	$Dec._{J2000}$ (°:′:″)	g' (mag)	i' (mag)	z (or v_r)	Object type
1	3C66A_01	02:22:35.3	42:59:05	22.275	20.518	0.3402 ± 0.0021	Elliptical
2	3C66A_02	02:22:35.7	43:00:32	21.849	21.309	0.0517 ± 0.0003	Spiral (strong bulge)
3	3C66A_03	02:22:50.7	43:01:03	18.859	17.830	0.1521 ± 0.0007	Spiral (Sa?)
4	3C66A_04	02:22:51.4	43:01:39	21.354	19.581	0.3390 ± 0.0004	Spiral
5	3C66A_05	02:22:34.9	42:59:58	22.012	20.974	...	Dwarf elliptical
6	3C66A_06	02:22:38.3	42:59:51	21.992	19.231	$(109.9 \pm 71.4\,km\,s^{-1})$	Galactic star
7	3C66A_07	02:22:44.1	43:01:28	21.827	20.575	0.5355 ± 0.0008	Spiral
8	3C66A_08	02:22:50.4	43:02:34	20.060	18.001	0.3402 ± 0.0006	Elliptical
9	**3C 66A**	02:22:39.6	43:02:08	14.323	13.755	...	Blazar
10	3C66A_10	02:22:51.3	43:02:52	21.489	20.559	0.4550 ± 0.0006	Irregular
11	3C66A_11	02:22:38.8	43:01:18	20.065	19.100	...	Dwarf elliptical
12	3C66A_12	02:22:40.2	43:02:20	21.828	19.730	0.3408 ± 0.0010	Elliptical
13	3C66A_13	02:22:26.7	43:01:42	21.138	19.768	...	Spiral or S0
14	3C66A_14[a]	02:22:50.4	43:03:47	18.124	17.072	0.0200 ± 0.0006	Dwarf elliptical
15	3C66A_15	02:22:35.1	43:02:09	22.116	19.933	0.3401 ± 0.0005	Elliptical
16	3C66A_16	02:22:39.4	43:03:04	21.383	19.247	0.3398 ± 0.0010	Elliptical
17	3C66A_17*	02:22:27.9	43:02:42	22.186	20.208	0.476 ± 0.0008	Spiral
18	3C66A_18	02:22:46.9	43:03:59	21.529	19.559	0.4930 ± 0.002	Early-type Spiral
19	3C66A_19	02:22:50.2	43:04:06	22.053	20.107	$(-83.0 \pm 9.5\,km\,s^{-1})$	Galactic star
20	3C66A_20*	02:22:35.4	43:03:53	21.579	20.107	0.479 ± 0.0007	Late-type spiral
21	3C66A_21	02:22:43.8	43:04:45	20.963	20.107	0.1755 ± 0.0003	Spiral (Sc?)
22	3C66A_22[b]	02:22:31.1	43:03:54	15.342	14.067	0.0201 ± 0.0007	Spiral (Sa)
23	3C66A_23	02:22:24.8	43:03:44	21.701	20.258	$(31.0 \pm 95.3\,km\,s^{-1})$	Galactic star
24	3C66A_24	02:22:32.6	43:02:18	21.710	20.478	0.4275 ± 0.0007	Spiral
- -	G2[c]	02:19:18.3	42:47:09	17.090	15.917	0.0667	Spiral

[a]Galaxy G3 in Bow97 (no redshift was reported).
[b]UGC 1832 ≡ galaxy G1 in Bow97; the published value $z = 0.0198$ agrees with our result.
[c]Redshift from Bow97.
*Galaxies whose tentative redshifts were measured through just one emission line.

results are shown in Table 1, where we also include the only galaxy with a previously published redshift within our GMOS field (G2 in Bow97).

3 RESULTS

In order to determine or – at least – to constrain the redshift of 3C 66A, we perform an individual spectroscopic analysis of the source itself, as well as a spectro-photometric analysis of its close environment, aiming to identify the host galaxy group of this BL Lac object. Considerations about the blazar's host galaxy are also presented.

3.1 Identification of galaxy groups

Based on the spectro-photometric results obtained (Table 1), we plot in Fig. 3 the distribution of the 18 spectroscopic redshifts measured within the area of our GMOS frame (17 from the this study plus one from the literature). We include eight additional galaxies with published redshifts (from NED) lying within 7 arcmin from 3C 66A, but out of our 5.5 × 5.5 arcmin field.

At least three concentrations of galaxies are evident in redshift space: one at $\langle z \rangle = 0.020$, the second at $\langle z \rangle = 0.067$ and the third one at $\langle z \rangle = 0.340$. The first (six members) is close to the redshift of the cluster Abell 347 ($z = 0.0184$; Abell 1958). In particular, the sightline to 3C 66A goes through the poor cluster WBL 069, associated to Abell 347, and composed by the galaxies UGC 1832, UGC 1837 and UGC 1841 (a.k.a. 3C 66B), and its compact dwarf

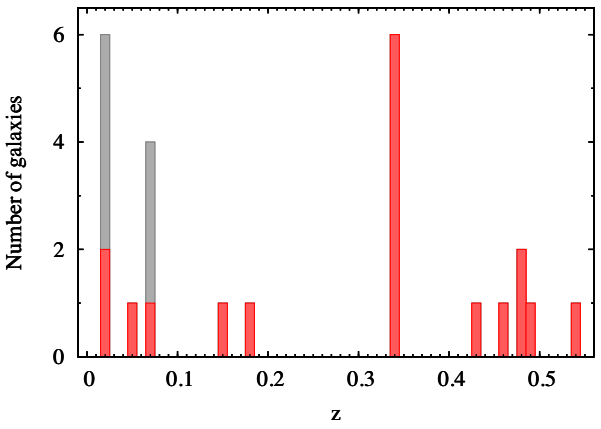

Figure 3. Redshift distribution of observed sources in a field of radius 7 arcmin centred on 3C 66A. Each bar represents the total number of objects with spectroscopic redshifts, both within (red) and outside (grey) the field studied in this paper. The histogram shows three galaxy groupings, at $z \approx 0.34$, $z \approx 0.067$ and at $z \approx 0.02$ in the close (projected) environment of the blazar.

neighbour V Zw 230, with a mean redshift $\langle z \rangle = 0.02088$ (White et al. 1999). UGC 1832 is galaxy G1 in Bow97; we obtain for it $z = 0.0201$ (slit #22), in agreement with the published redshift. We obtain $z = 0.0200$ for the galaxy in slit #14; Bow97 list this galaxy as G3, with no redshift value due to the low S/N in their spectrum. We thus confirm it as a member of the same foreground group.

A second group in redshift space comprises four galaxies within 5 arcmin from 3C 66A with redshifts between $z = 0.0674 \rightarrow 0.0677$ according to NED. These include galaxies G2, G4[6] and G6 in Bow97, along with the radio-source 3C 66, although only the first one lies within the GMOS field.

The third grouping is comprised by the six galaxies with redshifts between $z = 0.3390 \rightarrow 0.3402$ ($\langle z \rangle = 0.3400 \pm 0.0006$ rms) presented in this paper (see Table 1). They all have spectral features typical of early-type galaxies (see Fig. 4), while their magnitudes span between $g' \sim 20$ and 22.3 mag. Three of them are part of the galaxy overdensity identified by But76 in the immediate projected proximity of 3C 66A (see Fig. 2). In the following subsection, we shall further analyse the spatial distribution and location of these galaxies in the colour–magnitude relation (CMR).

Note that no galaxy was detected at $z \sim 0.444$, which is the usually quoted redshift for 3C 66A. This could be, at least partially, the result of a selection effect, given that an $M^\star$ elliptical galaxy would have $g' = 22.9$ mag at that redshift, i.e. too faint for our spectroscopy. However, we could still have measured spectroscopic redshifts for E galaxies with $M_{g'} \approx M^\star - 1$ mag at $z = 0.444$. Also note that our data were able to disclose four late-type galaxies at $0.43 < z < 0.54$; while none of them is exactly at the published redshift for 3C 66A, at least one of them (object #10 in Table 1) would lie within $\sim$3300 km s^{-1} of the blazar, if at that redshift. Thus, our spectroscopic data cannot either confirm nor rule out the presence of a cluster at $z = 0.444$ in the observed field.

3.2 The reference CRS as a clusters detector

Taking advantage of the evidence that early-type galaxies in rich clusters follow a linear CMR, called Cluster Red Sequence (CRS; e.g. Gladders & Yee 2000), and considering the universal properties that the CRS presents: a low-colour dispersion ($\sigma_{B-R} \sim 0.1$ mag; $\sigma_{g'-i'} \sim 0.04$ mag), a slope that does not change significantly with z, and a shift to redder colours as one progresses in redshift (López-Cruz et al. 2004), the CRS of a known cluster, or a reference CRS, can serve as a powerful observational tool for detecting galaxy clusters.

We use the red sequence of the Virgo cluster, conveniently shifted, as a reference CRS to confirm if the spectroscopically identified galaxies are members of galaxy clusters. At the same time, this allows us to identify new (photometric) candidate members for each cluster. The projected spatial distribution of both, confirmed and candidate members, may then provide additional support to a real connection between any of the clusters and the blazar.

The adopted CRS was obtained from the photometric analysis for 100 galaxies of the Virgo Cluster core performed by Chen et al. (2010), from SDSS (Sloan Digital Sky Survey) images in the *ugriz* bands. These galaxies allowed us to determine the best-fitting Virgo CRS, which is represented by

$$g' - i' = -0.0482\, g' + 1.6934. \quad (1)$$

We used this CRS shifted to $z = 0.34$ and 0.02 (Fig. 3). Shifts in $g' - i'$ colour and g' magnitude were established using K- and evolutionary corrections computed through the stellar population synthesis template galaxy models of Buzzoni (2005). We obtain for the Virgo red sequence at $z = 0.34$: $\Delta(g' - i') = 0.894$ mag and $\Delta g' = 10.33$ mag. Luminosity distance was computed with the aid of Ned Wright's *Cosmology Calculator*[7].

We plot in Fig. 5 the colour–magnitude diagram for all extended sources detected in the GMOS field of 3C 66A, showing also the Virgo red sequence shifted to $z = 0.34$ (blue solid line). The CRS clearly coincides with the position of the spectroscopically identified galaxies, confirming the presence of a cluster at $z \simeq 0.34$. To identify other candidate members of this cluster, we calculated a maximum colour scatter around the reference CRS and a magnitude limit to minimize effects from photometric errors and background contamination. The colour scatter was determined based on the six spectroscopically identified members, $\sigma_{(g'-i')} = 0.185$ mag. Following the recommendation of López-Cruz et al. (2004), the magnitude cut can be set at 2.0 mag below the apparent magnitude corresponding to the break of the typical cluster (Schechter) luminosity function, $M^*_R = -20.3 + 5 \log h$, at the cluster redshift. Given the adopted Cosmology, $M^*_R = -21.10$ mag. This magnitude was transformed into the Gunn-Sloan photometric system through the colours given by Buzzoni (2005) for galaxies of different ages, resulting in $M^*_{g'} = -20.26$ mag. Therefore, an appropriate magnitude cut can be set at $M_{g'} = -18.26$ mag, corresponding to $g' = 23.88$ mag for this cluster ($z = 0.34$). This allowed us to consider as probable members those objects with $g' < 23.88$ mag, which are within the $2\,\sigma_{(g'-i')}$ range of the CRS (blue dashed lines in Fig. 5). A total of 41 candidate members were identified in this way (including the six confirmed members), and we list them in Table 2. Galaxy 1456 (#18 in Table 1), however, is a background ($z = 0.493$) spiral whose colour is redshifted on to the $z = 0.34$ CRS. We consistently keep it in Table 2; it is clear that a certain level of contamination still remains within our candidate list.

Cluster membership probability for each galaxy was determined based on their magnitudes, following

$$P(g') = \frac{N(g') + N(g' < m < 23.88)}{N_{\rm T}}. \quad (2)$$

Here, $N(g')$ is the number of galaxies with apparent g' magnitudes within a given range, $N(g' < m < 23.88)$ is the number of galaxies with apparent magnitudes between the magnitude cut and g', while $N_{\rm T}$ is the total number of galaxies in the selected range. Besides membership probabilities, projected distances to the blazar (assuming they are at $z = 0.340$) were obtained for the 41 candidate members (see Table 2). Note that ≈50 per cent of the candidates would lie within 500 kpc (projected distance) from the blazar.

The spatial distribution of candidate members can be further illustrated by means of a density map (Gal et al. 2000). Fig. 2 shows contours of projected galaxy density, using a fixed Gaussian kernel with $\sigma = 1$ arcmin, where candidates are weighted by $P(g')$, as given in Table 2. The projected distribution of $z = 0.340$ candidates is strongly concentrated to 3C 66A, with the maximum density centred very close to the blazar. The central peak was found to be significant at a $>3\sigma$ level, through a significance map constructed from 500 synthetic data sets (see Gal et al. 2000, for details on significance maps computation).

The integrated luminosity of the 41 candidate member galaxies (excluding the blazar's host) amounts to $\mathcal{L}_{\rm tot}(g') = 3.4 \times 10^{11}\, \mathcal{L}_\odot$, giving an upper limit of total stellar mass $\mathcal{M}_\star \approx 5 \times 10^{12}\, \mathcal{M}_\odot$ (without considering any weight for the galaxies), consistent with a poor cluster of galaxies (see e.g. Buzzoni et al. 2012, and references therein), as proposed by Wurtz et al. (1993).

[6] This galaxy seems to be misidentified in NED; its coordinates in the data base point to an object that looks like a Galactic star.

[7] http://www.astro.ucla.edu/~wright/CosmoCalc.html (Wright 2006).

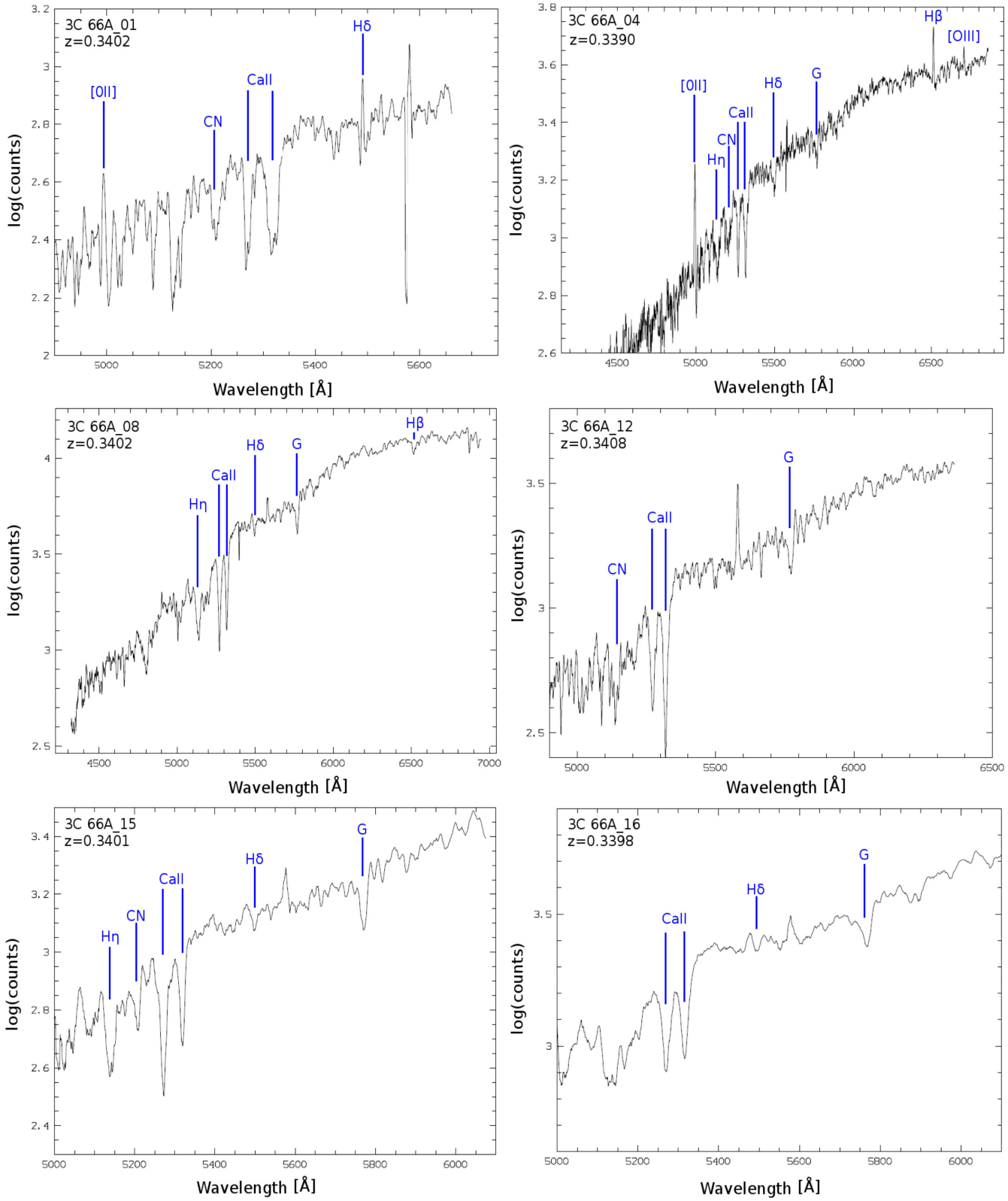

Figure 4. Optical spectra (*B*600_*G*5307 grating) of the six sources identified as group members at $z \sim 0.34$ within the field of 3C 66A, in units of counts per Ångstrom (no flux calibration was applied). Spectral features used to determine the redshifts of the sources are labelled. A few 'emissions' are residuals from poorly corrected sky lines.

Table 2. Membership probability of the candidate members of the cluster detected at $z = 0.340$: col. 1: identification label (ID) by SExtractor; cols. 2 and 3: RA and Dec. (J2000); cols. 4 and 5: g' and i' total integrated magnitudes; col. 6: membership probability; col. 7: projected distance to the blazar, if at $z = 0.340$ (the adopted cosmology gives a scale of 293.5 kpc arcmin^{-1}).

ID SExtractor	RA_{J2000} (hh:mm:ss)	$Dec._{J2000}$ (°:′:″)	g' (mag)	i' (mag)	$P(g')$	D_C (kpc)
872[#8]	02:22:50.4	43:02:34	20.06	18.00	1.000	593.0
1136	02:22:37.0	43:02:03	21.26	19.23	0.975	141.6
697[#4]	02:22:51.4	43:01:39	21.35	19.58	0.950	648.7
1377[#16]	02:22:39.4	43:03:04	21.38	19.25	0.926	274.1
1456[#18]	02:22:46.9	43:03:59	21.53	19.56	0.900	669.4
1195[#12]	02:22:40.2	43:02:20	21.83	19.73	0.878	66.9
717	02:22:47.1	43:01:22	21.89	19.97	0.853	461.0
1142	02:22:38.7	43:02:13	21.97	19.92	0.829	54.1
1243[#15]	02:22:35.1	43:02:09	22.12	19.93	0.800	241.4
1535	02:22:27.9	43:02:42	22.19	20.21	0.780	649.2
934	02:22:37.6	43:01:25	22.25	20.34	0.756	236.1
188[#1]	02:22:35.3	42:59:05	22.27	20.52	0.731	924.5
766	02:22:53.0	43:02:03	22.36	20.58	0.700	719.1
1006	02:22:39.8	43:01:58	22.43	20.48	0.682	50.1
1474	02:22:48.7	43:04:06	22.54	20.40	0.658	755.8
1082	02:22:40.7	43:02:07	22.57	20.33	0.634	59.2
1155	02:22:48.0	43:02:56	22.58	20.56	0.600	508.0
858	02:22:38.0	43:01:15	22.60	20.38	0.585	273.1
804	02:22:45.2	43:01:42	22.77	20.75	0.560	326.2
1372	02:22:38.1	43:02:50	22.94	21.10	0.536	220.6
2579	02:22:38.5	43:04:04	22.98	21.33	0.512	570.5
932	02:22:44.1	43:02:01	22.98	21.29	0.487	243.8
2081	02:22:38.3	43:04:18	23.00	20.93	0.463	639.7
772	02:22:38.1	43:00:53	23.01	21.17	0.439	375.7
1498	02:22:42.9	43:03:41	23.03	21.24	0.414	488.2
1388	02:22:36.1	43:02:44	23.04	21.26	0.390	257.4
1511	02:22:39.4	43:03:42	23.07	20.94	0.365	460.0
1111	02:22:49.1	43:02:52	23.20	21.38	0.341	553.1
2510	02:22:37.7	43:04:29	23.22	21.46	0.317	697.2
1910	02:22:23.7	43:03:23	23.22	21.43	0.292	928.2
198	02:22:46.4	42:59:59	23.24	21.16	0.268	729.0
1577	02:22:39.2	43:03:46	23.29	21.18	0.243	479.9
532	02:22:34.7	42:59:40	23.35	21.33	0.219	770.3
689	02:22:52.0	43:01:35	23.37	21.55	0.195	684.4
456	02:22:54.0	43:00:57	23.40	21.75	0.170	847.0
2478	02:22:44.6	43:04:50	23.47	21.55	0.146	836.6
1173	02:22:41.8	43:02:21	23.48	21.63	0.121	134.0
1936	02:22:27.6	43:03:39	23.69	21.93	0.097	782.4
2410	02:22:41.3	43:04:41	23.72	21.69	0.073	754.0
723	02:22:46.7	43:01:20	23.75	21.49	0.048	447.5
1553	02:22:28.3	43:02:42	23.81	21.85	0.024	628.4

#1, #4, #8, #12, #15, #16 and #18: object numbers in Table 1.

As discussed in Section 1, and considering that BL Lac objects are usually hosted by giant elliptical galaxies, typically associated with groups or galaxy clusters, we propose that the host galaxy of 3C 66A is a member of the cluster at $z = 0.340$ found in this work. Assuming that the host galaxy is typical for TeV emitting BL Lacs (see Section 3.4), its apparent magnitude should be $g' \sim 20.5$ mag, i.e. slightly fainter than the brightest galaxy in the group (slit #8). The cluster, then, seems to be dominated by these two bright ellipticals.

On the other hand, another red sequence, highlighted by some of the brightest objects in the field, can be visually identified in Fig. 5. We found that it can be fitted by shifting the Virgo CRS to $z = 0.02$, and the two galaxies with (spectroscopic) $z = 0.02$ lie on this red sequence; this allows us to verify the presence, within the analysed field, of several members of the foreground group associated with Abell 347. Note that the typical Abell radius for a galaxy cluster is 1.7 arcmin z^{-1}, so a cluster at $z = 0.02$ would cover a diameter of 170 arcmin. This indicates that the GMOS field of view (5.5×5.5 arcmin^2) allows us to observe only a small portion of the cluster (most probably at its outskirts). Since in this case we are sampling the faintest portion of the red sequence (where colour scatter is larger), in order to identify candidate members of this group we adopted a $(g' - i') = 0.16$ mag colour range (green dashed lines in Fig. 5), and a magnitude cutoff at $g' = 20.2$ mag, which corresponds to $M_{g'} = -14.5$ at $z = 0.02$, i.e. within the early-type dwarf galaxies domain, where the CMR is still well defined for nearby clusters (see Smith Castelli et al. 2008; Calderón et al. 2015). In this way, besides the two spectroscopically confirmed galaxies, #14 and #22, we identify **five** additional candidate members. Of these, galaxy G2 in Bow97 ($z = 0.0677$, i.e. a neighbour of the radio source 3C 66)

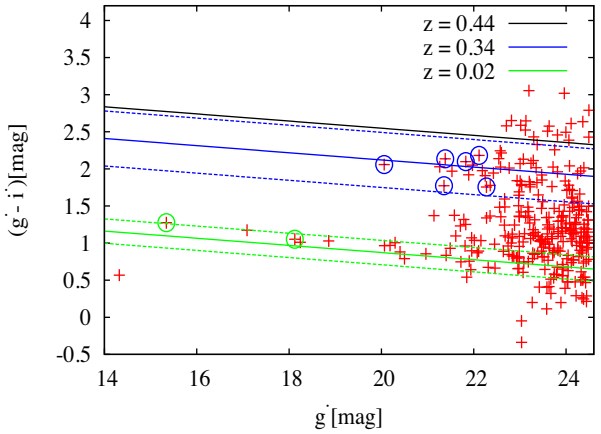

Figure 5. Colour–magnitude diagram (CMD) for detected galaxies in the field of 3C 66A (red crosses). Framed crosses within blue circles indicate the position of cluster members confirmed through spectroscopic redshifts ($z = 0.340 \pm 0.001$). The blue solid line shows the Virgo cluster CRS shifted to $z = 0.340$. Framed crosses within green circles indicate galaxies with spectroscopic redshifts $z \simeq 0.02$. The green solid line shows the Virgo cluster CRS shifted to $z = 0.02$. Dashed lines show the adopted colour scatter in each case. The black solid line shows the Virgo cluster CRS shifted to $z = 0.444$.

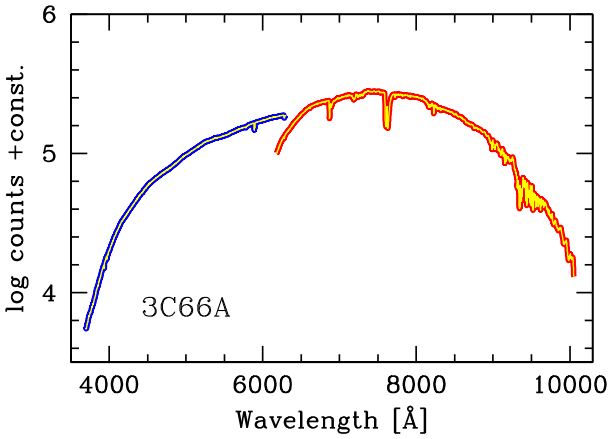

Figure 6. Wavelength branches of 3C 66A's spectrum. The branch obtained with the *B*600_*G*5307 grating (blue line) covers a spectral range between 3500 and 6500 Å, while the branch obtained with the *R*400_*G*5325 grating (red line) covers a spectral range between 6100 and 10 000 Å.

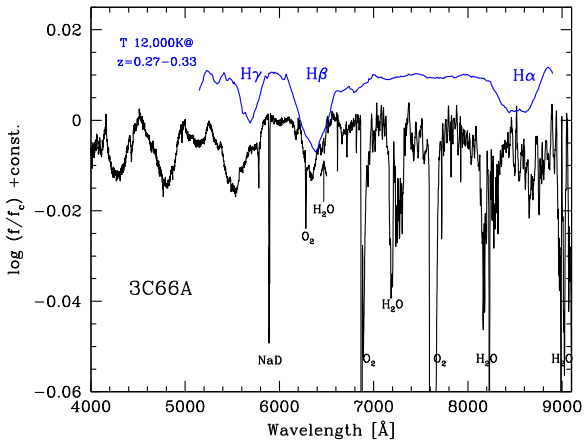

Figure 7. The linearized 3C 66A spectrum, compared with a BLUERED synthetic spectrum of a stellar model atmosphere with $T = 12\,000$ K shifted within the range $0.27 < z < 0.33$ (blue line). The Balmer sequence of the H γ, H β and H α absorption lines might be recognized to match the blazar spectrum. See the text for a discussion.

and object #3 ($z = 0.1521$) are background interlopers in the early-type galaxies CMR at $z = 0.02$. The other candidates (including objects #5 and #11, for which we could obtain no spectroscopic redshift, due to their very low surface brightnesses), however, show clear dE (dwarf elliptical) morphologies; this has been shown to be an excellent membership indicator for low-redshift clusters (e.g. Cellone & Buzzoni 2005, and references therein), so we retain them as probable members of the $z = 0.02$ group.

Note that no CRS for $z \sim 0.0677$ is evident in Fig. 5; the three galaxies at this redshift in Bow97 are spirals, so they may belong to a loose foreground grouping of late-type galaxies. We also show in Fig. 5 the Virgo CRS shifted to $z = 0.444$. No red sequence is observed at this z value down to $\sim M^{\star}$ ($g' = 22.9$ mag, see Section 3.1).

3.3 Analysis of the optical spectrum of 3C 66A

Due to its inherent nature of non-thermal emission, a proper analysis of any blazar spectrum is a difficult task. In our specific case, as we will see in the next section, the underlying galaxy hosting 3C 66A (most likely a gas-poor early-type system) seems to be too faint to leave any explicit signature in the target integrated spectrum. The resulting SED is, therefore, expected to lack any striking absorption feature, and actually this enhanced 'smoothness' is a recognized drawback when trying to constrain the blazar distance (and therefrom its related physical properties) through a redshift measurement.

A hint pointing to a quite 'blue' object does emerge from our photometry, once considering the likely effect of redshift on target apparent colour (namely, $g' - i' = 0.91$). The two wavelength branches of 3C 66A's spectrum, respectively, for the *B*600_*G*5307 and *R*400_*G*5325 gratings are displayed in Fig. 6.

At first glance, one sees that a more thorough analysis could be enabled if the bell-shaped instrumental response is removed, for instance by normalizing the observed spectrum with respect to its pseudo-continuum. This task has been carried out with the appropriate MIDAS routine (i.e. NORMALISE/SPECTRUM in the LONGSLIT context), by interactively identifying the upper envelope in the logarithmic count domain to be eventually subtracted to the observations. The blue and red branches of the spectrum have then been carefully matched around 6100 Å, and a unique spectrum, between 4000 and 10 000 Å, has been obtained (Fig. 7).

After linearization, a more entangled plot begins to appear from our data, clearly putting in evidence a number of thin but significant absorption features. To a closer analysis, one has to first report the pervasive contribution of telluric absorptions. Both O_2 and water vapour (H_2O) bands strongly affect the target emission and severely tackle our chance to single out any genuine target feature longward of ~7000 Å. The telluric pattern, however, fairly well compares with the study of Stevenson (1994) and these features clearly stand out, in our spectrum, for their sharp profile.

Quite more importantly, on the contrary, a number of broadened absorption features also mark the linearized spectrum, with prominent bands easily recognized about 4300, 4800, 5550, 6350 and 8700 Å (see, again, Fig. 7). Such broadened features are certainly of extragalactic origin, and might be suggestive of some interloping gas clouds, which selectively absorb the 3C 66A luminosity along the line of sight. No obvious constrain can be posed to this

scenario, of course, but a speculative fit with a redshifted synthetic spectrum from the BLUERED stellar library (Bertone et al. 2008) for a $T = 12\,000$ K (metal-poor) model atmosphere might lead to identify some of the observed bands with the H α, H β and H γ Balmer lines, as provided by foreground gas clouds up to $z \lesssim 0.33$, as sketched in the figure. If this is the real case, then a lower limit can be placed to 3C 66A redshift at $z_{3C66A} \gtrsim 0.33$.

3.4 The host galaxy

In this section, we briefly analyse the image of the blazar, in order to see if we can detect its host galaxy, to further constrain or confirm the blazar's redshift. We used IRAF task PSFMEASURE to fit a Moffat function to the PSF of the blazar and 12 stars on the central chip of the GMOS array (the same where the blazar image is). This was done on the g' image only, because in the i' image the AGN is slightly saturated. After correcting for PSF trends with position on the chip, we find that the *FWHM* of the blazar's PSF is marginally larger ($2.6\,\sigma$) than the mean value corresponding to stars. For the Moffat β parameter, in turn, the blazar's value is $4.0\,\sigma$ larger than for the stars. This would mean that the host galaxy is marginally resolved in our images, in agreement with Wurtz et al. (1996). However, the presence of haloes of stray light around the AGN and bright stars in our images makes this result uncertain.

We then simulated images of an elliptical galaxy (represented by a de Vaucouleurs model) with $M_R = -22.5$ mag and $R_{eff} = 10$ kpc (Sbarufatti et al. 2005; Shaw et al. 2013) plus a Moffat model representing the AGN, at different redshifts. Galaxy models 1 mag fainter/brighter than the mean adopted absolute magnitude were also considered, and their apparent magnitudes were calculated using *K*- and evolutionary corrections following Buzzoni (2005). Due to the mentioned stray light halo around the blazar's image, all we can say is that detection of a typical host galaxy at $z = 0.340$ would have been marginal, at best. In any case, it is clear that we can definitely rule out a low-redshift value such as $z = 0.067$, corresponding to the foreground grouping of galaxies mentioned in Section 3.1.

4 SUMMARY AND CONCLUSIONS

We have spectro-photometrically analysed the close environment of 3C 66A using two-band (g', i') optical images of a 5.5×5.5 arcmin^2 field centred on the blazar, along with multi-object spectroscopy obtained with the Gemini North telescope and the Gemini Multi Object Spectrograph. We obtained spectra for the blazar as well as 24 objects in the field, and we were able to measure reliable redshifts for 15 galaxies in the blazar's line of sight, spanning the range $0.02 < z < 0.53$. We found no evidence confirming the published redshift ($z = 0.444$) for 3C 66A, although we cannot formally rule it out either. Instead, we could firmly establish the presence of a galaxy group at $\langle z \rangle = 0.3400 \pm 0.0006$ in the close environment of 3C 66A. In particular:

(i) We identified two concentrations of galaxies (in redshift space) along the blazar line of sight, at $z \approx 0.020$ and 0.340, respectively. The first of them corresponds to the poor cluster WBL 069, associated to Abell 347 (White et al. 1999); we identified two new members of this cluster. The second one is composed of six objects with redshifts between $z = 0.3390$ and $z = 0.3402$; we classify almost all of them as early-type galaxies. On the other hand, there is a galaxy in our GMOS field which seems to belong to another loose grouping in the line of sight at $z \approx 0.067$, associated with the radio-source 3C 66.

(ii) Using the Virgo CRS (from data published in Chen et al. 2010) as a reference CRS, shifted to $z = 0.02$ and 0.34, we were able to identify two structures (i.e. 'red sequences') traced by early-type galaxies on the colour–magnitude diagram. The six galaxies with $\langle z \rangle = 0.340$ and the two galaxies with $\langle z \rangle = 0.020$, coincide with the position of the Virgo CRS shifted to these same z values, respectively, thus supporting the presence of two galaxy clusters, one at $z = 0.340$ and the other at $z = 0.020$.

(iii) Adopting a colour dispersion $\sigma_{(g'-i')} = 0.04$ mag for the cluster detected at $z = 0.02$, we identified seven candidate members (including two spectroscopically confirmed members and two confirmed background objects). On the other hand, for the $z = 0.34$ cluster, the colour dispersion (as measured from the six spectroscopically confirmed members) is $\sigma_{(g'-i')} = 0.185$ mag. This allowed us to identify 41 candidate members from the CMD (including six spectroscopically confirmed members and one confirmed background galaxy). The projected spatial distribution of $z = 0.340$ candidates shows a significant concentration centred on 3C 66A's position.

(iv) It was not possible to detect the 3C 66A host galaxy on the images. Simulations of a de Vaucouleurs profile for the host galaxy ($M_R = -22.5$ mag and $R_{eff} = 10$ kpc, Sbarufatti et al. 2005; Shaw et al. 2013) combined with a Moffat function for the AGN seeing convolved PSF, showed that the host galaxy would have been, at best, marginally detected if at $z = 0.34$. At the same time, membership of 3C 66A to any of the lower redshift groups at $z = 0.067$ and 0.020 can be ruled out.

(v) Analysing the blazar's normalized optical spectrum between 4000–10 000 Å, we were able to relate some absorption features with contributions of telluric origin, while shallow and broad absorption bands around 4300, 4800, 5550, 6350 and 8700 Å could be associated with the foreground intergalactic medium (IGM). By fitting a stellar synthetic spectrum ($T = 12\,000$ K) at varying redshifts, it was possible to tentatively identify those absorption bands with the Balmer series (H α, H β and H γ) produced in the IGM at $z \lesssim 0.33$. In this way, a redshift lower limit $z_{3C66A} \gtrsim 0.33$ can be established for 3C 66A. This is consistent with the firm lower limit $z \geq 0.3347$ and the 99.9 per cent confidence upper limit $z < 0.41$ given by Furniss et al. (2013).

Finally, considering these z lower/upper limits for 3C 66A, and taking into account the fact that BL Lac hosts are, typically, early-type galaxies associated to a group or a galaxy cluster (Urry et al. 2000), we propose that the host galaxy of 3C 66A belongs to a galaxy cluster at $z = 0.340$.

ACKNOWLEDGEMENTS

This paper is based on observations obtained at the Gemini Observatory (program GN-2009B-Q-2), which is operated by the Association of Universities for Research in Astronomy, Inc., under a cooperative agreement with the NSF on behalf of the Gemini partnership: the National Science Foundation (United States), the National Research Council (Canada), CONICYT (Chile), Ministerio de Ciencia, Tecnología e Innovación Productiva (Argentina), and Ministério da Ciência, Tecnologia e Inovação (Brazil). Data were acquired through the Gemini Science Archive and processed using the Gemini IRAF package.

This work has been partially supported with grants from La Plata National University (Argentina) and The Argentinian National Gemini Office. We thank Dr. Germán Gimeno, a Gemini staff member, for his advice in the process of Nod&Shuffle data

reduction, and Dr. Analía Smith Castelli for her recommendations on data analysis.

The authors want to thank the anonymous referee for valuable comments that really helped to improve this paper.

REFERENCES

Abell G. O., 1958, ApJS, 3, 211
Acciari V. A. et al., 2009, ApJ, 693, L104
Aliu E. et al., 2009, ApJ, 692, L29
Bertin E., Arnouts S., 1996, A&AS, 117, 393
Bertone E., Buzzoni A., Chávez M., Rodríguez-Merino L. H., 2008, A&A, 485, 823
Bowen D. V., Osmer S. J., Blades J. C., Tytler D., 1997, MNRAS, 284, 599
Bramel D. A. et al., 2005, ApJ, 629, 108
Butcher H. R., Oemler Jr A., Tapia S., Tarenghi M., 1976, ApJ, 209, L11
Buzzoni A., 2005, MNRAS, 361, 725
Buzzoni A., Cellone S. A., Saracco P., Zucca E., 2012, MNRAS, 420, 3427
Calderón J. P., Bassino L. P., Cellone S. A., Richtler T., Caso J. P., Gómez M., 2015, MNRAS, 451, 791
Cellone S. A., Buzzoni A., 2005, MNRAS, 356, 41
Chen C.-W., Côté P., West A. A., Peng E. W., Ferrarese L., 2010, ApJS, 191, 1
Costamante L., 2013, Int. J. Mod. Phys. D, 22, 1330025
Farina E. P., Fumagalli M., Decarli R., Fanidakis N., 2016, MNRAS, 455, 618
Finke J. D., Shields J. C., Böttcher M., Basu S., 2008, A&A, 477, 513
Furniss A., Fumagalli M., Danforth C., Williams D. A., Prochaska J. X., 2013, ApJ, 766, 35
Gal R. R., de Carvalho R. R., Odewahn S. C., Djorgovski S. G., Margoniner V. E., 2000, AJ, 119, 12
Gavazzi G., Zaccardo A., Sanvito G., Boselli A., Bonfanti C., 2004, A&A, 417, 499
Gladders M. D., Yee H. K. C., 2000, AJ, 120, 2148
Glazebrook K., Bland-Hawthorn J., 2001, PASP, 113, 197
González-Pérez J. N., Kidger M. R., Martín-Luis F., 2001, AJ, 122, 2055
Gould R. J., Schréder G. P., 1967, Phys. Rev., 155, 1404
Kennicutt Jr R. C., 1992, ApJS, 79, 255
Konigl A., 1981, ApJ, 243, 700
Landoni M., Falomo R., Treves A., Sbarufatti B., 2014, A&A, 570, A126
Landt H., 2012, MNRAS, 423, L84
Lanzetta K. M., Turnshek D. A., Sandoval J., 1993, ApJS, 84, 109
López-Cruz O., Barkhouse W. A., Yee H. K. C., 2004, ApJ, 614, 679
Maccagni D., Garilli B., Schild R., Tarenghi M., 1987, A&A, 178, 21
Mazin D., Raue M., 2007, A&A, 471, 439
Miller J. S., French H. B., Hawley S. A., 1978, BL Lac Objects. Pittsburgh Univ., Pittsburgh, p. 176; Discussion, p. 187
Muriel H., Donzelli C., Rovero A. C., Pichel A., 2015, A&A, 574, A101
Perri M. et al., 2003, A&A, 407, 453
Pesce J. E., Falomo R., Treves A., 1995, AJ, 110, 1554
Prandini E., Bonnoli G., Maraschi L., Mariotti M., Tavecchio F., 2010, MNRAS, 405, L76
Rovero A. C., Muriel H., Donzelli C., Pichel A., 2016, A&A, 589, A92
Sbarufatti B., Treves A., Falomo R., 2005, ApJ, 635, 173
Schlafly E. F., Finkbeiner D. P., 2011, ApJ, 737, 103
Shaw M. S. et al., 2013, ApJ, 764, 135
Smith Castelli A. V., Bassino L. P., Richtler T., Cellone S. A., Aruta C., Infante L., 2008, MNRAS, 386, 2311
Stecker F. W., de Jager O. C., Salamon M. H., 1992, ApJ, 390, L49
Stevenson C. C., 1994, MNRAS, 267, 904
Tonry J., Davis M., 1979, AJ, 84, 1511
Torres Zafra J., Cellone S. A., Andruchow I., 2013, Boletín de la Asociación Argentina de Astronomía, 56, 37
Urry C. M., Padovani P., 1995, PASP, 107, 803
Urry C. M., Scarpa R., O'Dowd M., Falomo R., Pesce J. E., Treves A., 2000, ApJ, 532, 816
White R. A., Bliton M., Bhavsar S. P., Bornmann P., Burns J. O., Ledlow M. J., Loken C., 1999, AJ, 118, 2014
Wright E. L., 2006, PASP, 118, 1711
Wurtz R., Ellingson E., Stocke J. T., Yee H. K. C., 1993, AJ, 106, 869
Wurtz R., Stocke J. T., Yee H. K. C., 1996, ApJS, 103, 109
Yan D.-H., Fan Z.-H., Zhou Y., Dai B.-Z., 2013, RAA, 13, 411
Yang J., Wang J., 2010, PASJ, 62, L23

This paper has been typeset from a TEX/LATEX file prepared by the author.